

7/28/92
E 7107

NASA Technical Memorandum 105713

Experimental Investigation of Wing Installation Effects on a Two-Dimensional Mixer/Ejector Nozzle for Supersonic Transport Aircraft

David J. Anderson, Heather H. Lambert, and Masashi Mizukami
*Lewis Research Center
Cleveland, Ohio*

LIMITED DISTRIBUTION DOCUMENT

Because of its significant technological potential, this information which has been developed under a U.S. Government program is being given a limited distribution whereby advanced access is provided for use by domestic interests. This legend shall be marked on any reproduction of this information in whole or in part.

July 1992

Date for general release July 30, 1995

NASA

EXPERIMENTAL INVESTIGATION OF WING INSTALLATION EFFECTS
ON A TWO-DIMENSIONAL MIXER/EJECTOR NOZZLE FOR
SUPERSONIC TRANSPORT AIRCRAFT

David J. Anderson, Heather H. Lambert and Masashi Mizukami
National Aeronautics and Space Administration
Lewis Research Center
Cleveland, Ohio 44135

SUMMARY

This report presents experimental results from a wind tunnel test conducted to investigate propulsion/airframe integration (PAI) effects. The objectives of the test were to examine rough order-of-magnitude changes in the acoustic characteristics of a mixer/ejector nozzle due to the presence of a wing and to obtain limited wing and nozzle flow-field measurements. A simple representative supersonic transport wing planform, with deflecting flaps, was installed above a two-dimensional mixer/ejector nozzle that was supplied with high-pressure heated air. Various configurations and wing positions with respect to the nozzle were studied. Because of hardware problems, no acoustics and only a limited set of flow-field data were obtained. For most hardware configurations tested, no significant propulsion/airframe integration effects were identified. Significant effects were seen for extreme flap deflections. The combination of the exploratory nature of the test and the limited flow-field instrumentation made it impossible to identify definitive propulsion/airframe integration effects.

INTRODUCTION

The next generation of supersonic transports will have to meet stringent noise levels specified under Federal Aviation Regulation (FAR) 36, stage III. To meet this noise regulation, the propulsion system concepts being explored today will require noise reduction techniques during takeoff. One possible jet noise reduction method is a high-entrainment ejector nozzle. The advantage of this concept is that by mixing low-velocity secondary air with the hot exhaust of the core engine, the lower resultant jet velocity and temperature produces less noise while minimizing thrust losses (ref. 1).

To improve mixing between the primary and secondary flows, a mixer primary nozzle could be added to the ejector to form the mixer/ejector nozzle concept. In this concept the cross section of the primary nozzle has convoluted lobes. The nonaxial discharge of the primary stream creates large-scale streamwise vorticity. This vorticity enhances the mixing of the primary and secondary flows. The principal advantage of the mixer/ejector concept is to entrain large amounts of secondary air and mix it with the hot primary flow in a short distance, resulting in a shorter and lighter nozzle. Ejectors being considered for this application have large entrainment weight flows. If the two flows are well mixed at the shroud exit, the mixed flow will have a significantly lower velocity and temperature than the primary airflow had when leaving the mixer nozzle. As with the straight ejector the lower velocity of the mixer/ejector's mixed flow produces less noise than primary flow alone would produce.

Installation of modern mixer/ejector nozzles on a nacelle/wing configuration of a supersonic transport aircraft has been shown to affect the flow field entering the nozzle's ejector inlets relative to an isolated mixer/ejector nozzle (refs. 2 to 4). The modified flow field approaching an ejector inlet

affects the ejector entrainment and the internal mixing characteristics of the nozzle. The resulting aeroperformance and acoustic characteristics of the propulsion/airframe system differ from those of the isolated components.

In the past, the propulsion system has been integrated onto an airframe after the independent development of each. Independent optimization of the propulsion system and airframe for supersonic transports often results in conflicting design requirements. The complex interactions dictate that propulsion/airframe integration (PAI) be addressed early in the development of both the propulsion system and the airframe.

The primary objective of the Propulsion/Airframe Integration for High-Speed Research-1 (PAIHSR1) wind tunnel test was to investigate changes to the acoustic characteristics of a two-dimensional mixer/ejector nozzle due to the influence of a wing on the nozzle flow. A secondary objective was to record a minimal set of wing and internal nozzle flow-field measurements for correlation with the acoustic data. Because of hardware problems discussed later, the acoustic measurements were not taken; only the flow-field measurements were recorded. The wing and nozzle flow-field data were examined for first-order PAI effects on the external flow field to the ejector inlets and on the internal flow characteristics of the nozzle. The PAIHSR1 test immediately followed an isolated test of the same two-dimensional mixer/ejector nozzle and used the existing nozzle hardware. This paper presents an analysis of the nozzle flow-field measurements and will discuss the effects that were seen and possibly why some effects were not observed.

Positioning and configuration effects of the wing with respect to the ejector inlets were studied during the PAIHSR1 test. Results are presented for various ejector inlet orientations, wing positions, leading- and trailing-edge flap settings and configurations, primary nozzle exhaust temperatures, and nozzle pressure ratios (NPR).

Flow-field measurements include surface static pressure measurements in the nozzle and on the wing and surveys of the total temperature and total pressure of the flow field at the nozzle's exit plane. Flow visualization of the wing's flow field was conducted by using yarn tufts. Pressure rakes were utilized on the wing to measure wing boundary layer changes.

Facility Description

NASA Lewis 9- by 15-Foot Low-Speed Wind Tunnel. - The 9- by 15-Foot Low-Speed Wind Tunnel (LSWT) test section was built in the return leg of the 8- by 6-Foot Supersonic Wind Tunnel at the NASA Lewis Research Center (fig. 1; ref. 5). The facility is an anechoic wind tunnel and was designed for measuring aerodynamic and acoustic data on aircraft and propulsion components under low-speed conditions. The test section is 2.95 m (9 ft) high by 4.92 m (15 ft) wide by 8.86 m (27 ft) long (ref. 6). The tunnel's walls, ceiling, and floor consist of modular acoustically treated boxes and are removable to allow test hardware mounting and data measurement flexibility.

The maximum nominal test section Mach number is 0.2. The tunnel total temperature and pressure reflect outside ambient conditions. The high-pressure air system for the facility can supply 3.102-GPa (450-psi) pressure air at temperatures up to 505 K (910 °R) (ref. 6).

Jet Exit Rig. - The jet exit rig (JER) is a strut-and-body apparatus for testing exhaust nozzles that require hot or cold high-pressure airflows. Heated air is provided by the facility for moderate temperatures or is heated by a combustor in the JER for high temperatures. The warmed facility air

temperature is limited by the temperature capability of the force balance and seals. An axisymmetric gaseous hydrogen and air combustor is used to produce hot gases up to 1264 K (2200 °R). Cooling water is necessary to cool the combustor section when burning hydrogen for the hot flows. The JER was originally intended to support hot exhaust flow requirements that were needed for valid acoustic measurements during the isolated-nozzle test. A combustor failure at the end of the isolated-nozzle test precluded acoustic testing during the PAIHSR1 portion of the mixer/ejector nozzle test. The use of only the warmed facility air did allow for the testing of a greater number of configurations.

Figure 2 shows an artist's rendering of the JER with a round conic checkout nozzle. The two parallel air supplies are transitioned into two coannular flows. The inner airflow is used for combustion; the outer airflow can be used as a bypass flow. The maximum weight flow to the nozzle, for one or two separate flows, is 15.9 kg/sec (35 lb/sec). Only the internal heated flow stream was used for the PAIHSR1 test; the bypass flow was blocked off. NPR's of 1.0 to a maximum of 6.0 can be achieved.

An axisymmetric nozzle can be bolted directly behind the axisymmetric combustor. Mounting a two-dimensional nozzle requires a round-to-two-dimensional transition section. Figure 3 shows the JER with a Pratt & Whitney mixer/ejector nozzle mounted in the LWST. For this test the JER's angle-of-incidence capability was not used. The JER is too long and will produce a boundary layer that will not match one from an appropriately sized nacelle (as matched to the nozzle). The JER is still adequate to provide a first-order representation of a nacelle for this test.

HARDWARE DESCRIPTION

Mixer/Ejector Nozzle

Description. - The mixer/ejector nozzle concept tested was the result of a cooperative program between Pratt & Whitney and NASA Lewis. The primary nozzle is a two-dimensional, eight-lobed mixer nozzle combined with an ejector section (fig. 4). The ejector shrouds consist of two aerodynamically designed sections positioned symmetrically about the nozzle centerline and opposite the lobes. The two shrouds are attached to two sideplates that are bolted to the sides of the primary nozzle.

Three shroud lengths were designed, and the shortest and longest shrouds were used during the PAIHSR1 test. The shrouds were instrumented with rows of static pressure taps and thermocouples. Both short shrouds were instrumented, but only one of the long shrouds was instrumented. The primary nozzle exit was at approximately 11 percent chord of the short shroud. The sideplates required cutouts on the front portions of the plates for the PAIHSR1 test to allow for aft wing positioning without hitting the sideplates.

Figures 5(a) and (b) show the wing above the JER in the LSWT, with the nozzle in its two different orientations. Figure 5(a) shows the nozzle with its ejector inlets on the top and bottom with respect to the wing. This nozzle orientation will be referred to as "the vertical orientation." Figure 5(b) shows the wing with its ejector inlets on the sides with respect to the wing. This nozzle orientation will be referred to as "the horizontal orientation." All data presented in this report will be addressed by their orientation to the wing (inboard or outboard, top or bottom) or by which side (A or B) of a set of primary nozzle lobes it is on (fig. 6).

Nozzle Asymmetry. - A nozzle asymmetry was identified through analysis of the data and later by physical measurement of the primary nozzle. Although this should not alter any PAI effects experienced

during the test, it does preclude direct comparison of opposite shroud static pressures and opposite halves of a traverse survey plot.

Figures 6 and 7 show the effect of the nozzle asymmetry on the opposite shroud static pressures and the nondimensional temperature contours at NPR's of 2.5 and 3.5, respectively. Only minor effects are shown in the data for an NPR of 2.5. The NPR=3.5 data show a noticeable asymmetry effect on the opposite shroud static pressures and on the exit total temperature contours. The difference in the magnitude of the effect between NPR's is due to the greater momentum of the primary flow for the NPR=3.5 case.

PAIHSR1 Wing

The wing consisted of a flat, tapered-plate center section with wedge-shaped leading- and trailing-edge flaps. The leading- and trailing-edge sweep angles and the flap geometry are representative of a supersonic transport. The wing was designed to generate a leading-edge vortex and to approximate flap flow fields. The wing was installed at a 5° angle of attack in order to ensure formation of the leading-edge vortex. Ingestion of the leading-edge vortex at takeoff and approach conditions could affect the ejector performance. Figure 8 shows a two-view drawing of the wing mounted above the jet exit rig and the nozzle. The position of the JER in the tunnel and the distance between the support strut and the ejector inlets were two critical dimensions in the design of the wing. The distance of the JER from the wall was dictated by the isolated-nozzle test. As a result of these constraints the size of the JER was not compatible with the size of the wing, but the wing still generated the principal flow characteristics of interest. The wing was of similar scale to the nozzle in order to match the relative scales of the flow fields.

The general wing planform was recommended by the NASA Langley Research Center, and the actual wing and positioning hardware was designed and fabricated in house at NASA Lewis. Figure 9 shows the key dimensions of the wing and the short interfairing. The wing planform was based on previous supersonic transport designs developed and tested at Langley.

The wing had simple hinged leading- and trailing-edge flaps. The flaps were hinged at the lower surface of the wing, and the upper surface attachment was made by using curved metal plates with different-length arcs for the various flap deflections. Two key benefits of this approach were that flap deflection could be changed quickly and that the pressure instrumentation did not have to be disconnected to make the changes. Both sets of flaps (leading edge and trailing edge) were deflected during the test.

Two interfairings, the segment between the two trailing-edge flap sections and directly above the JER, were designed and independently tested. The long interfairing is shown in figure 5. A short interfairing was tested with the vertical nozzle orientation; it was 6.35 cm (2.5 in.) long with a lower surface parallel to the wing's lower surface (fig. 9). A full-length interfairing might have blocked off a significant portion of the upper ejector inlet when the wing was moved aft. Because a blockage of this type is not a valid installation for this nozzle design, the short interfairing was devised.

The position of the wing with respect to the ejector inlets was varied. An actuated X-Y table was used to mount the wing to the tunnel wall and to allow for fore and aft movement, as well as a vertical adjustment of the wing above the ejector inlets. The X-Y table also had a splitter plate mounted to it in order to divert the tunnel wall's boundary layer away from the wing. Figure 10 shows the matrix of X and Y values for 18 wing positions, as well as their relative positions with respect to the ejector inlet.

The positioning of the wing is based upon the point of the wing's trailing edge above the JER centerline. The standard wing position matrix consists of wing positions (WP) 1 to 15. The most forward positions (WP5, 6, and 15) were determined by setting the wing's trailing-edge point directly above the beginning of the ejector inlet. The most aft positions (WP1, 10, and 11), of the standard wing position matrix were determined by the outboard trailing edge of the long interfairing and the cutout made in the sideplates. The outboard tip of the long interfairing hit the outboard vertical sideplate 4.75 cm (1.875 in.) before the trailing-edge point would reach the end of the ejector inlet. WP16 to 18 represent the furthest aft the X-Y could travel and were used to represent ejector inlets ahead of the flaps in a possible real installation.

The vertical positions of the wing were based upon three factors: The first was in maintaining a minimum clearance of 2.54 cm (1 in.) between the maximum thickness of the JER (the combustor section) and the lowest point of the wing (the interfairing hinge line). The minimum Y value of 1.9 cm (0.75 in.) reflects a difference in height between the maximum diameter of the JER and that of the entrance of the ejector inlet. Second, the desired maximum height was to be one equivalent nozzle diameter, approximately 15.3 cm (6 in.). A mechanical height limit was experienced prior to one full equivalent nozzle diameter; the maximum change in height was limited to 13.35 cm (5.25 in.). Third, the middle height was to be approximately one-half of the equivalent nozzle diameter above the minimum height.

INSTRUMENTATION

The following instrumentation were installed on the wing. Forty-three static pressure taps were on the wing surface: three rows on the upper side, and two rows on the lower side (fig. 11). Both the short and long flap interfairings had static pressure taps: three on the short, and four on the long. Two boundary layer rakes were placed on the lower surface of the wing just upstream of the nozzle, and one boundary layer rake was placed on the upper surface of the short flap interfairing. These help to determine the effect of the ejector entrainment on the wing flow. The rakes were 7.35 cm (2.87 in.) tall, with 10 total pressure probes each. Yarn tufts were attached to the wing surface, and their patterns were viewed from several different angles and recorded on videotape.

The following nozzle instrumentation was available: There were static pressure taps on the inner side of the ejector shrouds, one row parallel to a peak (centerline of a lobe) of the primary nozzle and one row parallel to a center valley (midpoint between two lobes) (fig. 12). Both short shrouds were instrumented in this way, but only one of the long shrouds was instrumented. There were pressure taps and thermocouples on the inner (primary) and outer (secondary) sides of the lobed primary nozzle (fig. 13). At the shroud exit a total temperature and total pressure rake on a horizontal traverse mechanism was used to obtain exit plane total temperature and total pressure contours. The rake had 15 equally spaced probes for each measurement and was 9.35 cm (3.75 in.) tall. However, as shown in figure 4, the traverse rake did not cover the entire exit area.

Test Configurations

Table I presents combinations of the hardware configurations and primary flow conditions tested. The elements of the hardware configuration that could be varied were nozzle orientation, interfairing length, shroud length, leading- and trailing-edge flap settings, and wing position. Six different hardware configurations were tested at various wing positions for a specified set of primary-flow NPR's. The nominal primary-flow NPR's were 1.0, 1.4, 1.7, 2.5, 3.0, 3.5, and 4.0.

The column headings of the matrix, shown in Table I, define the six combinations of nozzle orientation, interfairing and shroud length, and flap settings tested. The wing positions, defined in figure 9, are listed in the left column of the matrix. Data were recorded for those hardware configuration/wing position combinations marked with an asterisk at wind tunnel conditions of Mach 0.2 and ambient temperature and nozzle conditions of 429 K (700 °R) primary-flow temperature for the set of NPR's given earlier. Limited data were also obtained at ambient wind tunnel conditions (Mach 0.0, ambient temperature) for the set of NPR's at ambient and 429 K (700 °R) primary-flow temperatures.

Parametric studies of the shroud and interfairing length were done with the nozzle ejector inlets oriented vertically. Both the leading- and trailing-edge flaps were set to zero for these parametric studies. The effects of shroud length were investigated with the short interfairing. The short interfairing was used because the long since the long interfairing blocked the ejector inlet and hence was unrealistic with the vertical ejector inlet orientation. The effects of interfairing length were investigated with the short shrouds because both shrouds were instrumented.

Another parametric study of the effects of varying flap setting was done with the ejector inlets oriented horizontally. The long interfairing and the short shrouds were used for this study. The long interfairing was flush with the wing trailing edge at 0° flap deflection, which is a more realistic configuration for the horizontal nozzle orientation. Three sets of leading- and trailing-edge flap deflections were investigated: leading- and trailing-edge flaps at 0° (0/0, the baseline wing configuration); leading-edge flaps at 0° and trailing-edge flaps at 20° (0/20); and leading-edge flaps at 20° and trailing-edge flaps at 40° (20/40). Because of exploratory nature of the test and a short test window, the sets of flap deflections were selected to cover a wide spectrum of possible effects. The flap deflections investigated do not reflect operational configurations.

As previously stated, the effects of varying wing position were investigated for all six different hardware configurations described earlier. The standard set of wing positions tested were 1, 3, 5, 6, 8, 10, 11, 13, and 15. Additional wing positions tested, as time was available, were 2, 16, 17, and 18.

Temperature and total pressure rakes, behind the nozzle in figures 4 and 5(a), were traversed across the nozzle exhaust flow for selected test conditions. The Taguchi orthogonal array technique (ref. 7) for the design of experiments was applied to the test variables to determine the minimum number of traverse runs. A limited number of additional traverse runs were performed to allow for some direct comparisons.

RESULTS

Two types of plots are presented in this section: shroud static pressure ratio ($P_s/P_{t,0}$) versus the ratio of the distance back from the shroud leading-edge to the chord of the shroud (X/C), and nondimensional total temperature contours at the shroud exit. The nondimensional total temperature contours reflect the surveyed temperatures of the exhaust. The temperature contours are based upon the tunnel ambient (with the minimum contour value of 0.0) and primary nozzle exhaust (with the maximum contour value of 1.0) total temperature. Complete mixing would produce widely spaced contours with a narrow range of contour values.

Five wing positions (WP1, 5, 8, 11, and 15) were selected as representative. NPR's of 2.5 and 3.5 were selected as representative. The majority of the data presented in this report is for these representative conditions. Other wing positions are addressed as warranted.

Effect of Wing Position With Vertical Ejector Inlets

Effect of WP on long shroud. - The first configuration that was used to study the effect of wing position on the ejectors was with the long shroud, short interfairing, leading- and trailing-edge flap settings at 0° , and vertical nozzle orientation. The standard set of wing positions was tested at the nominal NPR's. Figures 14 to 16 show the shroud static pressures and temperature contours for the long shroud at NPR's of 2.5 and 3.5. Figures 14 to 16 show that the position of the wing had no noticeable effect on the shroud static pressures or the total temperature contours.

Effect of WP on the short shroud. - The second configuration that was used to study the effect of wing position on the ejectors was with the short shroud, short interfairing, leading- and trailing-edge flap settings at 0° , and vertical nozzle orientation. The standard set of NPR's and wing positions, plus WP2, was used. Figures 17 to 19 show the shroud static pressures and the total temperature contours for the short shroud at NPR's of 2.5 and 3.5. At the wing positions examined, no effects of varying wing position were noticed. Figure 17(b) presents the shroud pressures recorded on the top shroud for the five representative wing positions at an NPR of 3.5. The shroud pressures for all wing positions closely matched those recorded for the isolated-nozzle case.

Figures 14 to 19 show that the position of the wing had no noticeable effect on the shroud static pressures or the total temperature contours for either shroud length. The differences between the total temperature contours for the short and long shrouds were purely a function of the length of the mixing region, and not any integration effect.

Effect of Interfairing Length for Two Wing Positions

The configurations that were used to study the effect of interfairing (IF) length on the ejectors were the short shroud, leading- and trailing-edge flap settings at 0° , and vertical nozzle orientation, with both the short and long interfairings. The standard set of NPR's was tested at two wing positions (WP1 and 5) for the long interfairing, and the standard set of NPR's and WP's was tested for the short interfairing. Figure 20 shows static pressures for the top schroud at NPR's of 2.5 and 3.5. There was no effect from either of the two different interfairing lengths on the shroud static pressures with the vertically oriented ejector inlets for WP1 and WP5. No traverse surveys were conducted for the long interfairing with the vertically oriented ejectors.

For WP5, the most forward and lowest position of the wing, the results were not unexpected. For WP1, the most aft and lowest position tested, some effect of interfairing length was anticipated because the long interfairing would cover the majority of the top ejector inlet in the plan view. A geometric limitation for the lowest wing positions, as discussed later, may explain why there was no effect of interfairing length for WP1. At WP1 the wing was still 4.3 cm (1.7 in.) above the top ejector inlet. We believe that ejector pumping is maintained as long as the wing is a suitable height above or ahead of the top ejector. If the wing were positioned closer to the top ejector inlet than WP1, the top ejector inlet may experience an effect that could be measured by the static pressures on the top shroud.

The effect of interfairing length for horizontal ejector inlets was not studied during this test. Intuitively, changes in interfairing length for this nozzle orientation should have no noticeable effect on the nozzle's ejector inlet flow.

Effect of Wing Position With Flaps for Horizontal Ejector Inlets

The third configuration that was used to study the effect of wing position was with the long inter-fairing, short shroud, and horizontal nozzle orientation, with all three sets of flap deflections. The standard set of NPR's and wing positions were tested. Shroud internal pressures and exit temperature contours at representative NPR's of 2.5 and 3.5 were analyzed.

Flaps 20/40. - At flap setting 20/40, significant effects of different wing positions on the nozzle were observed. At this flap setting the flow over the trailing-edge flaps appeared to be separated. For WP3 and WP5 and both NPR's, unusually low inboard shroud pressures were observed at the leading edge of the inboard shroud (fig. 21). At these wing positions the trailing-edge flaps were placed directly adjacent to and upstream of the ejector inlets. This effect was most likely due to the low-pressure separated region or the flap trailing-edge vortex impinging on the shroud. Note that at WP1 the flap trailing edge was well downstream of the ejector inlets and therefore this effect was not seen.

For most other wing positions a lower static pressure was measured behind the inboard shroud leading edge. This decrease could potentially be caused by a change in flow direction due to the wing and the trailing-edge flaps, separated flow behind the trailing-edge flaps, flow disturbance due to the leading-edge flaps, vortices from the trailing-edge flaps, or interacting flow between the trailing-edge flaps and the flap inter-fairing. Furthermore, the pressure changes relative to wing position were different for varying NPR, indicating that the type of fluid dynamics involved and the particular external flow features ingested depend on the amount of secondary pumping.

For NPR=2.5 most of the pressure decrease was near the leading edge, and the inboard shroud pressures were only slightly lower than isolated-nozzle ones (fig. 22(a)). WP18 showed the greatest pressure decrease just aft of the leading edge and a smaller decrease further aft. WP1 had the smallest pressure decrease. For NPR=3.5 the inboard shroud pressures behind the leading edge were significantly lower than for an isolated nozzle (fig. 22(b)). The greatest decrease was seen for WP1, and the smallest for WP11 and WP18. No significant effect was observed on the outboard shroud pressures, possibly because the flap flow was directed away from the ejector inlets by the overall outward flow under the wing.

Exit temperature contours showed that the hotspots changed position and intensity depending on wing position. Relative to the isolated nozzle (figs. 6(c) and 7(c)), the inboard hotspots were displaced significantly further inboard and slightly downward, and the centerline hotspot moved somewhat inboard and down for NPR=3.5 and WP1 shown in figure 23(a). This effect was much more pronounced for NPR=3.5 than for NPR=2.5. The greatest displacements occurred for WP1 and WP8. Also for these cases the inboard lower hotspots were actually hotter than for the isolated nozzle, possibly due to the flap partially obstructing the ejector inlet.

At WP5, slightly improved mixing was observed in the exit temperature contours for both NPR's (figs. 23(b) and (c)). In general, the hotspots were cooler and more diffuse than those seen in the isolated-nozzle contours. It is speculated that the turbulence in the flap separated flow, or the strong streamwise vorticity of the flap trailing edge, entering the ejector inlets could have actually improved the internal mixing. However, the effect of this flow on the overall nozzle thrust is unknown.

Flaps 0/0 and 0/20. - At flap settings of 0/0 and 0/20, only minor wing position effects were observed. At both NPR's, 0/20 flaps, and WP5, a low-pressure region at the leading edge was measured (fig. 24), similar to the kind described previously. For other wing positions a small increase in static

pressure was observed behind the leading edge. With flaps at 0/0, only slight wing position effects were seen on the shroud pressures. No appreciable effects were observed on the exit temperature contours for either flap setting.

Effect of Flap Setting at Selected Wing Positions for Horizontal Ejector Inlets

The following configuration was used to investigate the effect of varying leading- and trailing-edge flap settings: horizontal nozzle orientation, long interfairing, and short shroud. Three sets of leading- and trailing-edge flap deflections were tested: leading- and trailing-edge flaps at 0° (0/0); leading-edge flaps at 0° and trailing-edge flaps at 20° (0/20); and leading-edge flaps at 20° and trailing-edge flaps at 40° (20/40). Figure 25 shows shroud pressures recorded on the inboard shroud for the isolated nozzle and the available sets of flap deflections for different NPR's and wing positions. The shroud static pressure ratios are plotted as a function of shroud chord length.

Figures 25(a) and (b) show shroud pressures recorded at WP1 and NPR's of 2.5 and 3.5, respectively. In general, the shroud pressures recorded for leading-edge/trailing-edge deflections of 0/0 and 0/20 were the same as the shroud pressures recorded for the isolated nozzle for all NPR's and wing positions.

At flap deflections of 0/0 (the baseline wing configuration) it is not surprising that the pressures matched the isolated-nozzle case. The flow over and under the wing should be attached. Because the jet exit rig was not mounted onto the wing, there were no pylon effects. No unusual flow phenomena were generated near the ejector inlets, other than those generated by the presence of the wing itself, such as changes in flow direction and the presence of wing boundary layers. It is not possible to determine from the available data whether the flow into the ejectors came from the sides of the JER or from the region between the JER and the wing. In either case the presence of the wing had a negligible effect.

At flap deflections of 0/20 the flow field around the wing and the JER changed from that generated by the baseline wing configuration. A vortex was probably generated at the inside edge of the outboard trailing-edge flap. A second vortex was probably generated at the outside edge of the inboard trailing-edge flap. One vortex was probably generated at each of the inboard and outboard edges of the interfairing. The presence of these vortices is inferred from general aerodynamic principles coupled with the limited experimental data. The vortices induced on the trailing-edge flaps by the interfairing may bypass the ejector inlets or may be ingested without affecting the shroud pressures (figs. 25(a), (b), and (d)). At WP5 the pressures at the leading edge of the shroud (chord 0.0 to 0.05) were lower than those for the isolated-nozzle and 0/0 flap deflection cases. This may be due to impingement of a vortex or simply accelerated flow around the leading edge.

The shroud pressures recorded at flap deflections of 20/40 differed significantly from the other cases, indicating the entrainment of flow phenomena generated by the 20/40 flap deflections. Several changes occurred in the flow field. The deflection of the leading-edge flaps affected the flow above the wing, and more importantly, below the wing and between the JER and the wing. The flow over the trailing-edge flaps was separated, and hence had lower static pressure. The previous discussion on the four vortices still applies, although the characteristics of each vortex may be different.

Shroud pressures for the 20/40 flap deflections were lower than for the other configurations, at all NPR's and wing positions (fig. 25). The magnitude of the pressure decrease and the chord area affected varied with NPR and WP. In general, the magnitude of the pressure decrease and the chord area affected increased with primary-flow NPR for a given wing position (figs. 25(a) and (b)). The variation with

wing position is discussed in the section on wing position effects. Figures 25(a) and (b) are representative of the differences in shroud pressures recorded for most wing positions.

As before, the specific cause of the pressure decrease cannot be identified from the available data. For the isolated nozzle at $\text{NPR} > 2.5$ the flow around the leading edge of the shroud was supersonic, followed by a shock located near 10 percent of the shroud chord. At $\text{NPR} = 3.5$ and WP1 (fig. 25(b)), the pressure profile for flap deflections of 20/40 could result from accelerated flow near 0.1 to 0.13 X/C , followed by a shock at or near 0.13 X/C , with higher pressures downstream of the shock. Increased flow velocity would imply increased secondary flow. Similarly, the pressure profile for flap deflections of 20/40 at $\text{NPR} = 2.5$ could have resulted from accelerated flow and increased secondary flow, although the flow for the isolated nozzle at $\text{NPR} < 2.5$ remained subsonic throughout the nozzle. In the absence of vortices, low-pressure separated flow, and modified flow between the wing and JER, the pressure decrease would indicate increased pumping through the ejector inlet. However, the nonuniform nature of the flow near the ejector inlets suggested that the pressure decrease probably resulted from the entrainment of a vortex, a separated flow, or a modified flow between the JER and the wing, and most probably some combination of all three.

The pressures for two wing positions (WP5 and 18) showed different trends than those for the other wing positions. The pressures at the leading edge of the shroud for WP5 and 20/40 flap deflections were lower than those for the isolated-wing and 0/0 flap deflection cases (fig. 25(c)). The effects mentioned for the 0/20 flap deflection case may explain the lower pressures, but a definitive explanation cannot be derived from the available instrumentation. At WP18 the pressures were higher than those for the other wing positions (fig. 25). At this wing position the trailing-edge flaps were low and aft, and a smaller area of the ejector inlet was exposed to the separated flow.

The effect of flap deflection on exit temperature contours was examined for WP1 and WP5 and NPR 's of 3.5 and 2.5. The effects varied with wing position and NPR . Exit temperature contours at WP1 and NPR 's of 2.5 and 3.5 differed from the isolated-nozzle case for all the sets of flap deflections. At flap deflections of 20/40 the hotspots shifted inboard and downward significantly. In general, the effects were small and it is impossible to determine the overall effect on mixing and nozzle performance. Figure 26 shows exit temperature contours at WP5 and $\text{NPR} = 3.5$ for the isolated-nozzle case and flap deflections of 0/0, 0/20, and 20/40; these contours are also representative of the effects recorded at $\text{NPR} = 2.5$. At WP5 and NPR 's of 2.5 and 3.5 the exit temperature contours for 0/0 and 0/20 flap deflections showed lower temperatures in some regions of the nozzle exit relative to the isolated-nozzle case (figs. 26(a) to (c)). At 20/40 flap deflections, both NPR 's of 2.5 and 3.5 showed significant decreases in temperature relative to the isolated-nozzle case (figs. 26(a), and (d)). The temperature decreases indicate an improvement in mixing. Again, the overall effect on nozzle performance cannot be determined from the available data.

DISCUSSION

Of the wing positions investigated, the lower positions (WP1, 3, 5, and 18) better represented the relative positions of the wing and the nozzle. Although the use of the wing positioning table allowed for a parametric variation of wing location with respect to the nozzle, the wing was decoupled from the nozzle and the jet exit rig. This decoupling may have missed some very important integration effects. The importance of these effects were understood but were not addressed in this test in order to allow for the easy parametric variation in wing position, which was a focus in this test. And although the 20/40 flap setting produced noticeable effects, it probably did not create a realistic flap flow, owing to separation.

The entrainment of the modern mixer/ejector nozzles is an order of magnitude, or more, greater than that experienced by the ejector nozzle concepts explored in the past. These higher entrainment flows may be less susceptible to the same integration effects, which did produce noticeable effects on the lower entrainment ejectors (refs. 2 and 3). The lack of noticeable measured effects from this test on the shroud static pressures and exit temperature contours for the two NPR's discussed in this report does not contradict this possibility.

On an actual aircraft the nozzle will be integrated with the wing and the PAI effects may be potentially greater than for the PAIHSR1 test configuration. The nacelle may be attached to the wing with a pylon, or it may be directly attached to the wing with a flow diverter; in other words, air cannot flow across the bottom of the wing between the wing and the nacelle, and the wing/pylon boundary layer effects become much more significant. Also, the flaps may be larger and closer to the ejector inlets.

The quality of any integration data set is highly dependent on the amount and location of the instrumentation. Because this test was designed as an addition to an existing isolated-nozzle test, the desired instrumentation for determining the fluid dynamics of the wing/flap flow entering the mixer/ejector nozzle could not be installed. To draw firm conclusions regarding these PAI effects, better flow visualization and flow-field instrumentation are required. The PAIHSR1 test provided valuable experience in terms of learning instrumentation requirements needed for PAI testing and where care needs to be taken in terms of the integration parameters.

CONCLUDING REMARKS

A wind tunnel test to investigate propulsion/airframe integration (PAI) for supersonic transport aircraft was conducted. The primary objective of the wind tunnel test was to investigate changes to the acoustic characteristics of a two-dimensional mixer/ejector nozzle due to the influence of a wing on the nozzle flow. A secondary objective was to obtain a minimal set of wing and internal nozzle flow-field measurements for correlation with the acoustic data. Owing to hardware problems, the acoustic measurements were not taken: only the flow-field measurements were recorded. The wing and nozzle flow-field data were examined for first-order PAI effects on the external flow field to the ejector inlets and on the internal flow characteristics of the nozzle.

The test was conducted in the NASA Lewis 9- by 15-Foot Low-Speed Wind Tunnel. Heated high-pressure air was supplied to a two-dimensional mixer/ejector nozzle. A simplified wing, with a planform representative of a supersonic transport, was placed immediately above the nozzle. The parameters varied were axial and vertical wing position, leading- and trailing-edge flap deflections, nozzle orientation, nozzle pressure ratio, flap interfairing length, and nozzle shroud length. Shroud internal static pressures and exit total temperature contours were presented.

For most of the hardware configurations tested, no significant PAI effects were identified from the available instrumentation. Minor variations in shroud pressures and exit temperature contours were observed as a result of varying wing position, nozzle orientation, interfairing length, and shroud length and moderate flap deflections. Significant effects were seen for extreme flap deflections. Specifically, substantial changes occurred in shroud static pressures, both internally and at the leading edge. The position and intensity of exit temperature contour hotspots changed as well.

This test resulted in a limited set of PAI data for a two-dimensional mixer/ejector nozzle that was designed for use on supersonic transports. Problems with large flap deflections were highlighted in the data. The combination of the exploratory nature of the test and the limited flow-field instrumentation

made it impossible to identify definitive PAI effects. The flow field in the region of interest is very complex and highly coupled; detailed analysis will require a highly instrumented and integrated test configuration. A more closely integrated configuration with realistic geometries may have had a greater effect on the nozzle internal flow field and acoustics. Propulsion/airframe integration effects are still expected to significantly impact the performance and acoustics of mixer/ejector nozzles. Further study and testing are required to develop a more complete understanding of PAI effects.

ACKNOWLEDGMENTS

The authors would like to thank John Wolter of NASA Lewis for his technical support; Chris Domack of Lockheed for support on the wing; and Chris Jones of Pratt & Whitney for technical assistance.

REFERENCES

1. Lord, W.K., Jones, C.W., Stern, A.M., Head, V.L. and Krejsa, E.A., "Mixer Ejector Nozzle for Jet Noise Suppression," AIAA Paper 90-1909, July 1990.
2. Stitt, L.E., "Exhaust Nozzles for Propulsion Systems With Emphasis on Supersonic Cruise Aircraft," NASA RP-1235, 1990.
3. Mikkelson, D.C., and Head, V.L., "Flight Investigation of Airframe Installation Effects on a Variable Flap Ejector Nozzle of an Underwing Engine Nacelle at Mach Numbers From 0.5 to 1.3," NASA TM-X-2010, 1970.
4. Atencio, A., Jr., "The Effect of Forward Speed on J85 Engine Noise From Suppressor Nozzles as Measured in the NASA-Ames 40- by 80-Foot Wind Tunnel," NASA TN D-8426, 1977.
5. Yuska, J.A., Diedrich, J.H., and Clough, N., "Lewis 9- by 15-Foot V/STOL Wind Tunnel," NASA TM-X-2305, 1971.
6. Krejsa, E.A., Cooper, B.A., Hall, D.G., and Khavaran, A., "Noise Measurements From an Ejector Suppressor Nozzle in the NASA Lewis 9- by 15-Foot Low Speed Wind Tunnel," NASA TM-103628, (Also, AIAA Paper 90-3983, Oct. 1990).
7. Ross, P.J., Taguchi Techniques for Quality Engineering, McGraw-Hill Book Company, New York, 1988.

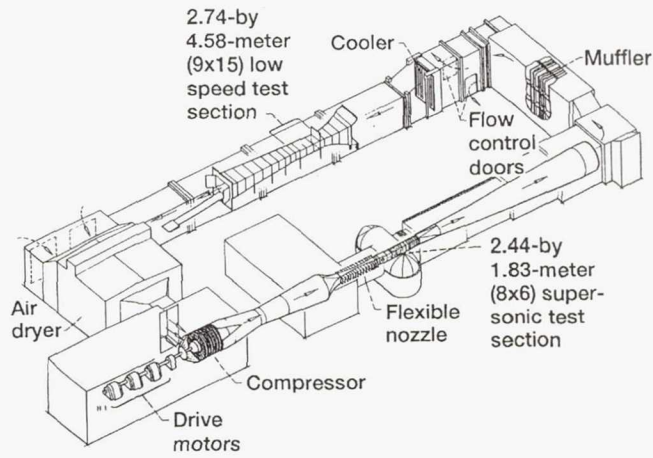


Figure 1.—NASA Lewis 9- by 15-Foot/8- by 6-Foot Wind tunnel complex.

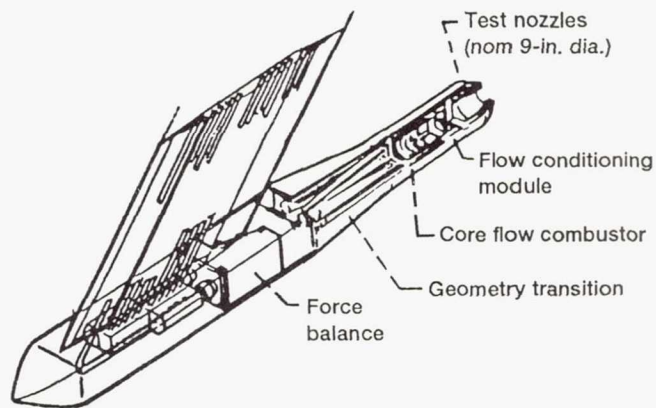


Figure 2.—Jet exit rig with transition for axisymmetric nozzles.

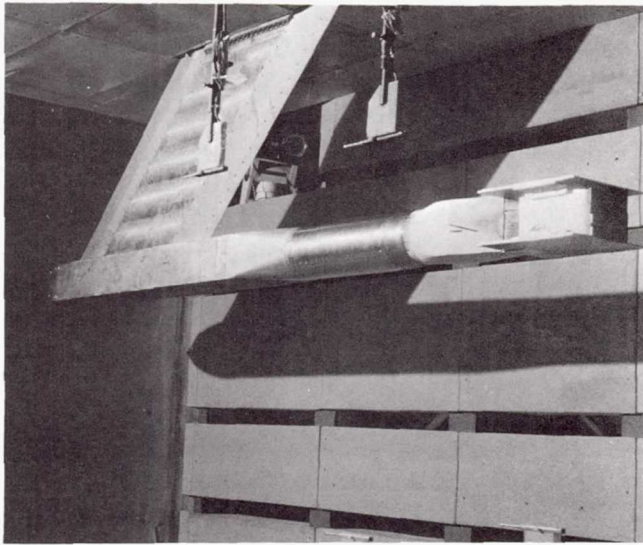


Figure 3.—Jet exit rig mounted in NASA Lewis 9- by 15-Foot Wind Tunnel with Pratt & Whitney two-dimensional mixer/ejector nozzle.

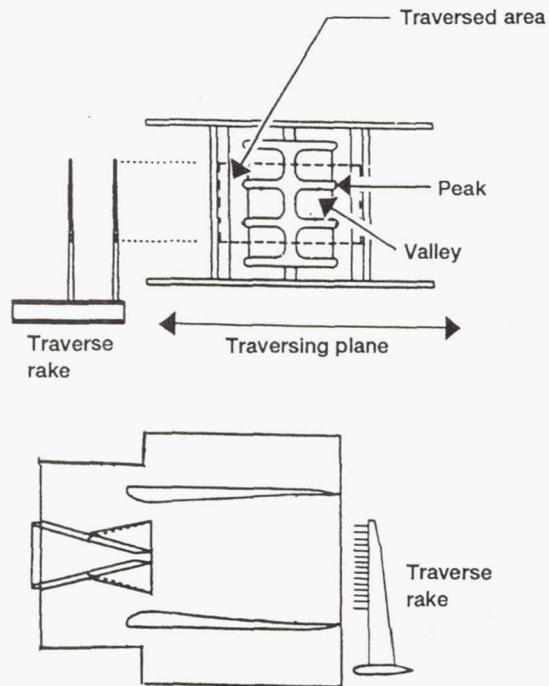
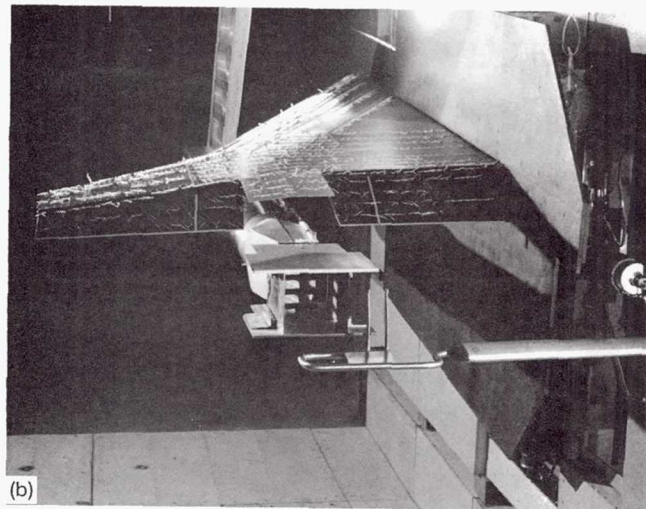
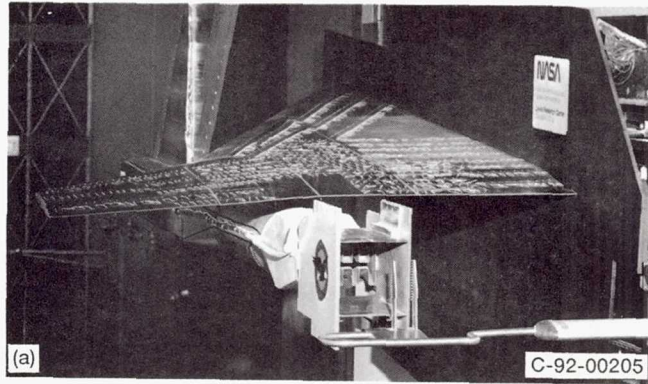


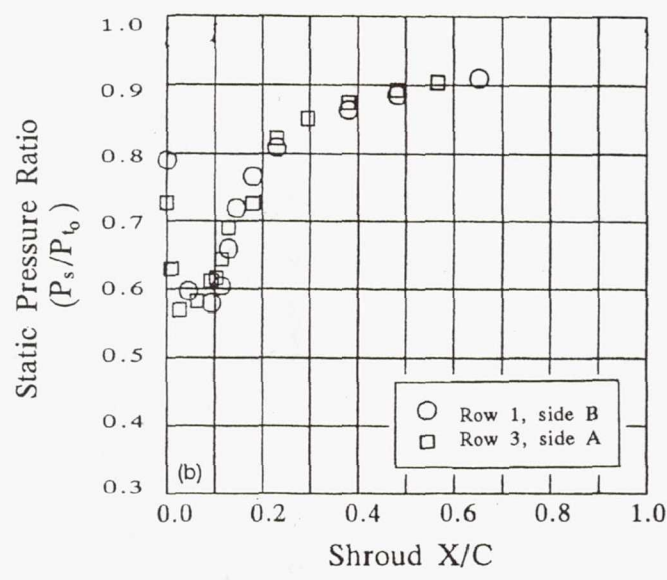
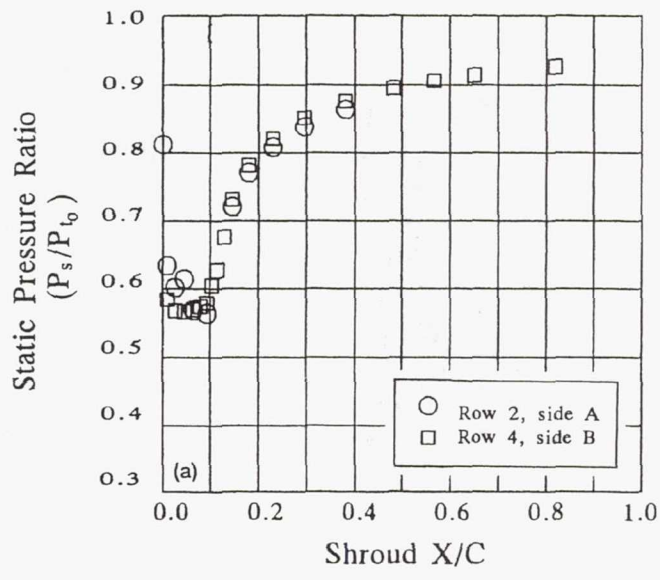
Figure 4.—General layout of Pratt & Whitney two-dimensional mixer/ejector nozzle with short shroud and exit traverse rake.



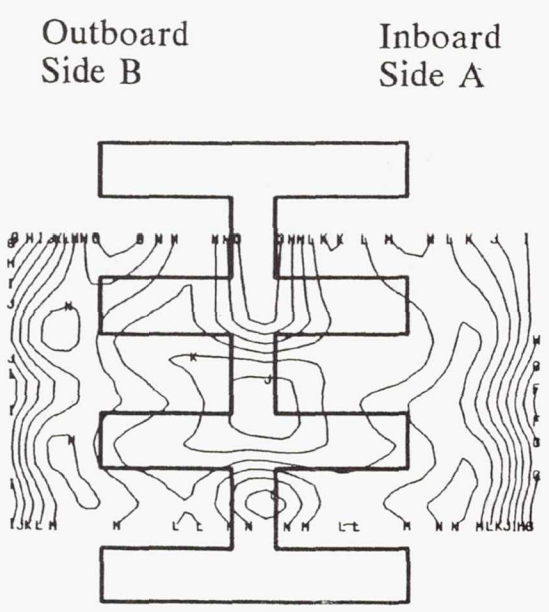
(a) Nozzle in vertical orientation.

(b) Nozzle in horizontal orientation.

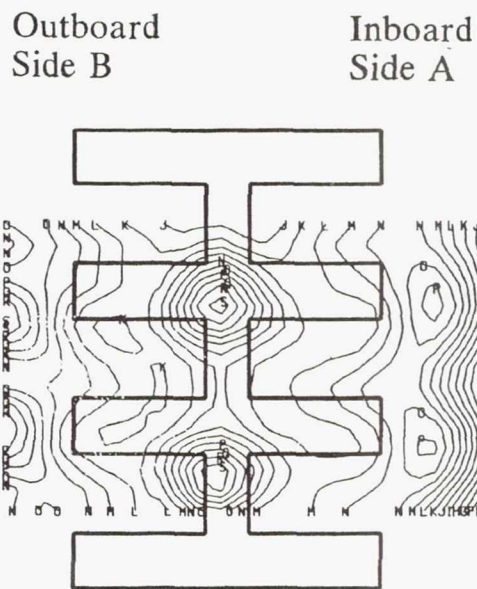
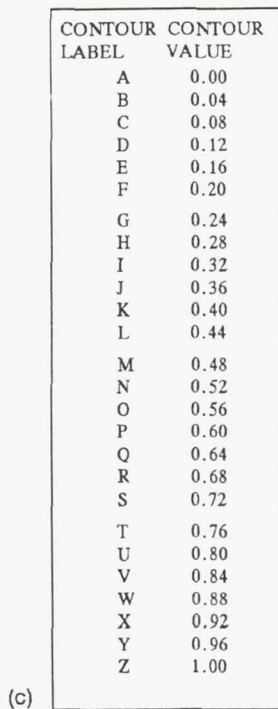
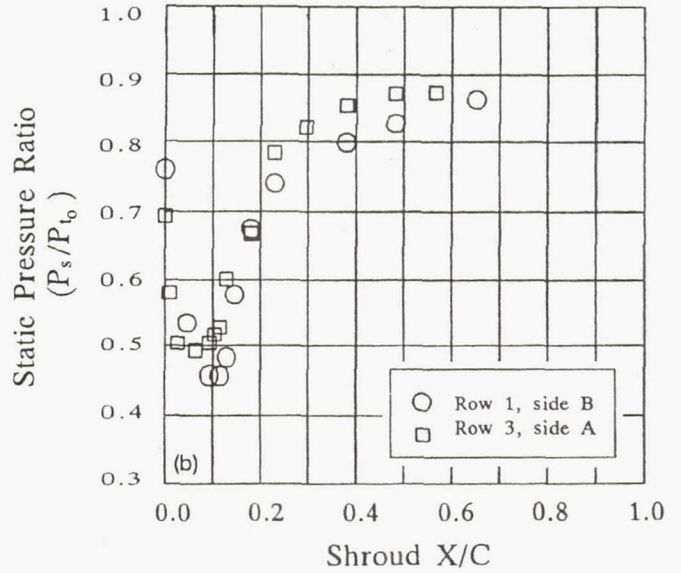
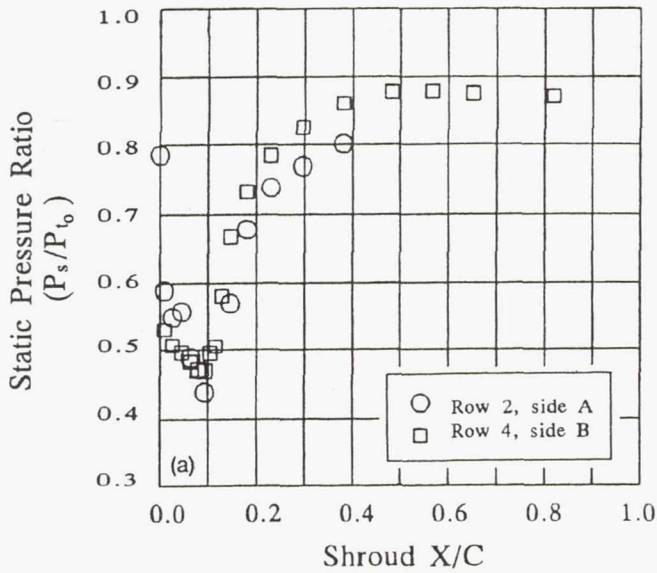
Figure 5. - PAIHSR1 wing mounted above jet exit rig and nozzle.



CONTOUR LABEL	CONTOUR VALUE
A	0.00
B	0.04
C	0.08
D	0.12
E	0.16
F	0.20
G	0.24
H	0.28
I	0.32
J	0.36
K	0.40
L	0.44
M	0.48
N	0.52
O	0.56
P	0.60
Q	0.64
R	0.68
S	0.72
T	0.76
U	0.80
V	0.84
W	0.88
X	0.92
Y	0.96
Z	1.00



(a) Shroud pressures over peaks of primary nozzle.
 (b) Shroud pressures over valleys of primary nozzle.
 (c) Nondimensional total temperature contours.
 Figure 6. - Isolated-nozzle shroud pressures and total temperature contours for nozzle pressure ratio of 2.5.



(a) Shroud pressures over peaks of primary nozzle.
 (b) Shroud pressures over valleys of primary nozzle.
 (c) Nondimensional total temperature contours.
 Figure 7.—Isolated-nozzle shroud pressures and total temperature contours for nozzle pressure ratio of 3.5.

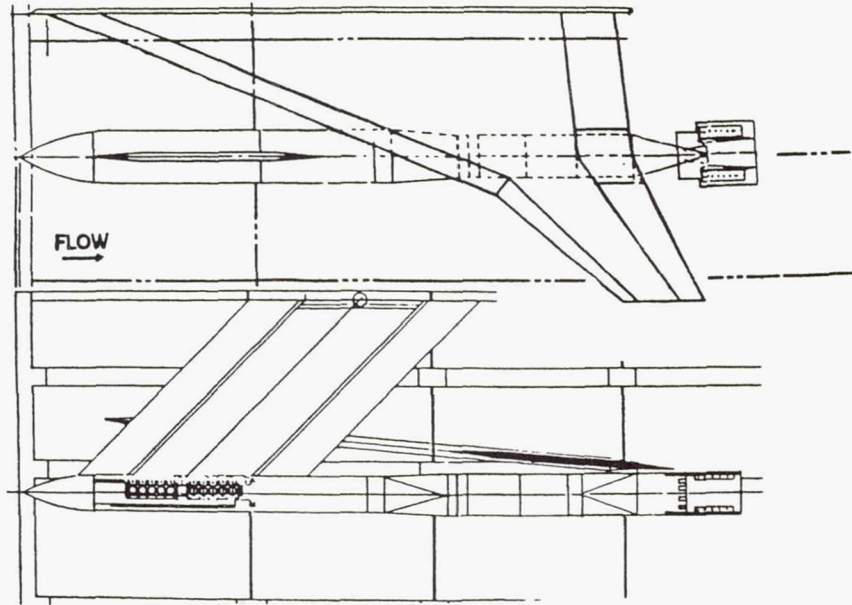


Figure 8.—Schematic of PAIHSR1 wing above jet exit rig and mixer/ejector nozzle.

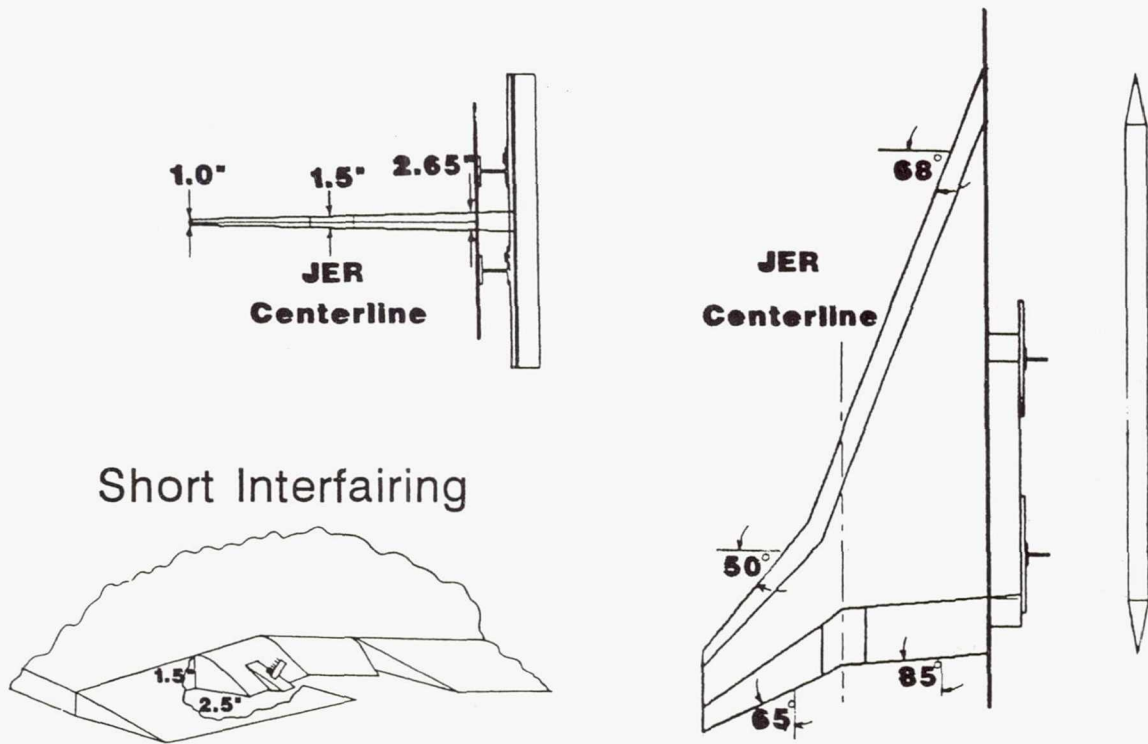


Figure 9.—Key dimensions of PAIHSR1 wing and short interfairing.

Wing Position	X position	Y position	Wing Position	X position	Y position
1	-12.75	0.75	10	-12.75	3.75
2	-9.0	0.75	11	-12.75	6.0
3	-6.375	0.75	12	-9.0	6.0
4	-3.0	0.75	13	-6.375	6.0
5	0.0	0.75	14	-3.0	6.0
6	0.0	3.75	15	0.0	6.0
7	-3.0	3.75	16	-17.0	6.0
8	-6.375	3.75	17	-17.0	3.75
9	-9.0	3.75	18	-17.0	0.75

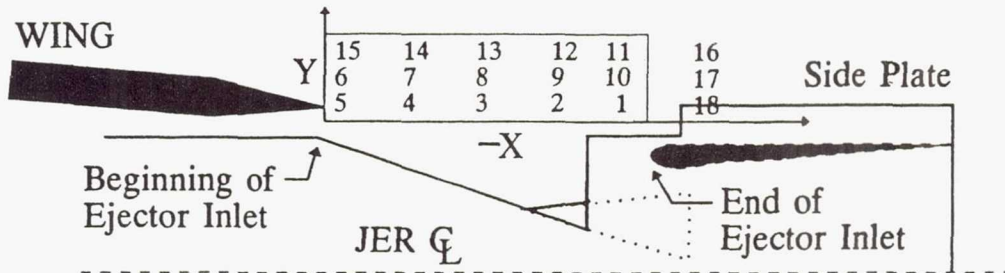


Figure 10.—Wing positions and matrix schematic.

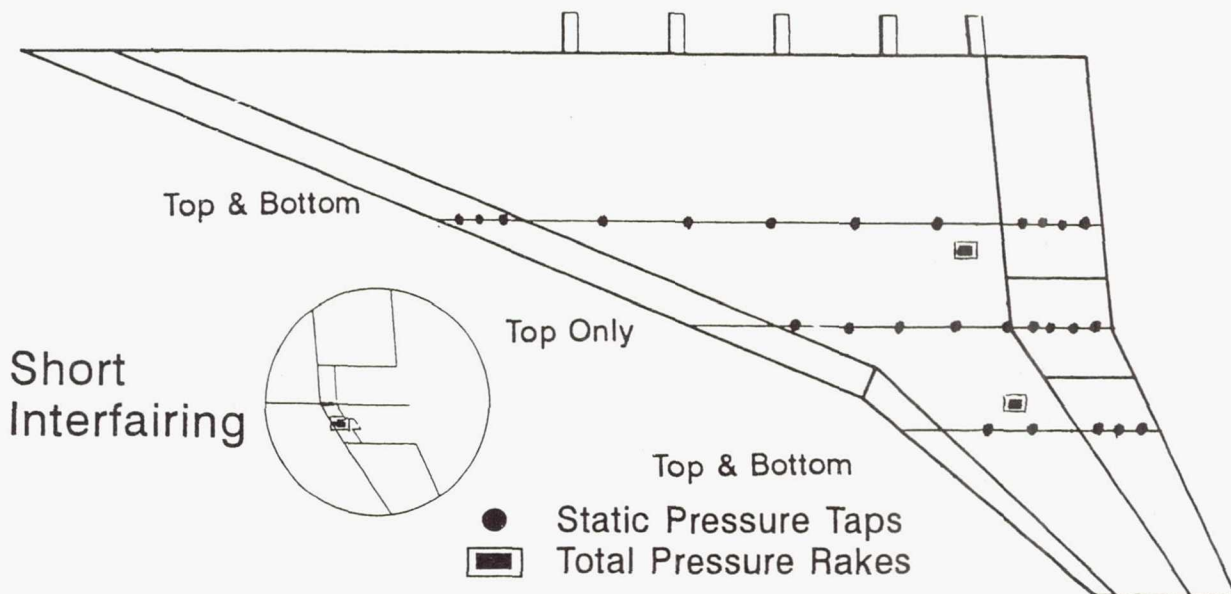


Figure 11.—PAIHSR1 wing static pressure and total pressure rake locations.

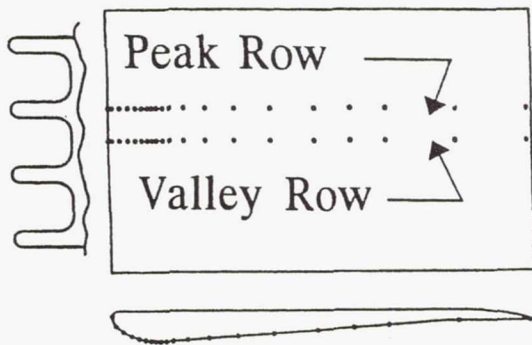


Figure 12.—Shroud static pressure instrumentation.

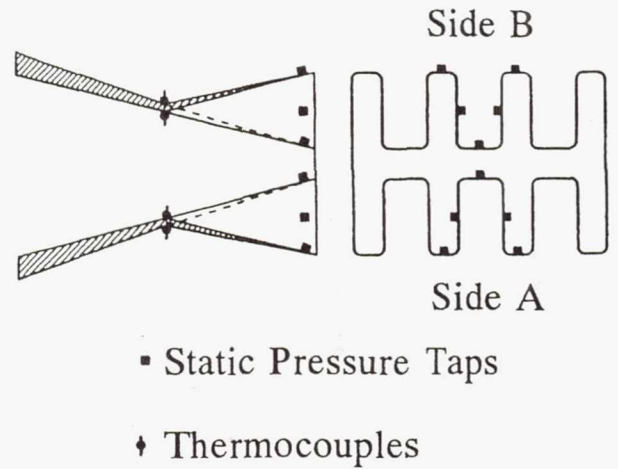
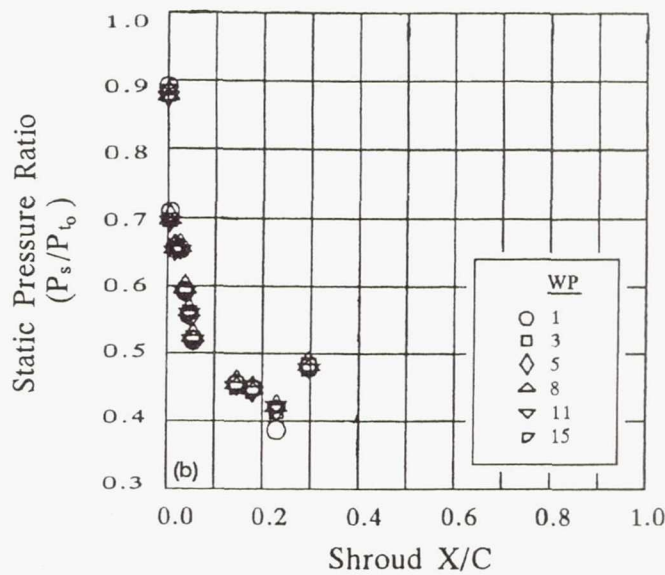
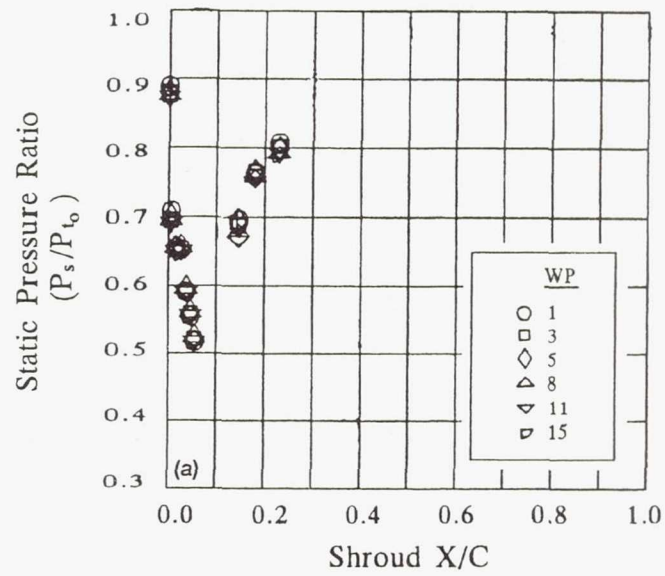


Figure 13.—Primary nozzle static pressure and thermocouple locations.

Wing Position	Ejector Orientation		Side/Side			Top/Bottom		
	Interfairing		Long			Short		Long
	Shroud		Short			Short	Long	Short
	Flap Settings (LE/TE)		0 deg/0 deg	0 deg/20 deg	20 deg/40 deg	0 deg/0 deg	0 deg/0 deg	0 deg./0 deg.
1		
2		
3		
4		
5		
6		
7		
8		
9		
10		
11		
12		
13		
14		
15		
16		
17		
18		

TABLE I.—TEST CONFIGURATION MATRIX

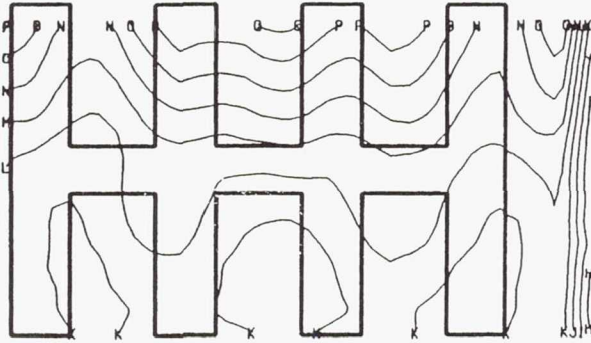


(a) NPR=2.5.

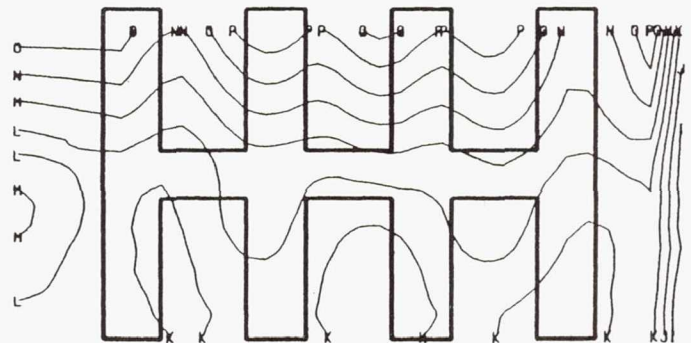
(b) NPR=3.5.

Figure 14.— Long-top-shroud static pressures for six wing position.

CONTOUR LABEL		CONTOUR VALUE			
A	0.00	G	0.24	M	0.48
B	0.04	H	0.28	N	0.52
C	0.08	I	0.32	O	0.56
D	0.12	J	0.36	P	0.60
E	0.16	K	0.40	Q	0.64
F	0.20	L	0.44	R	0.68
				S	0.72
				T	0.76
				U	0.80
				V	0.84
				W	0.88
				X	0.92
				Y	0.96
				Z	1.00



(a)

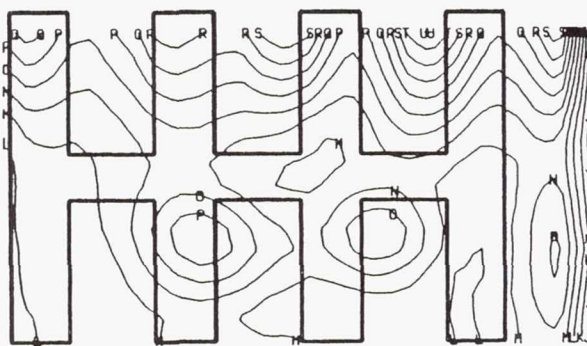


(b)

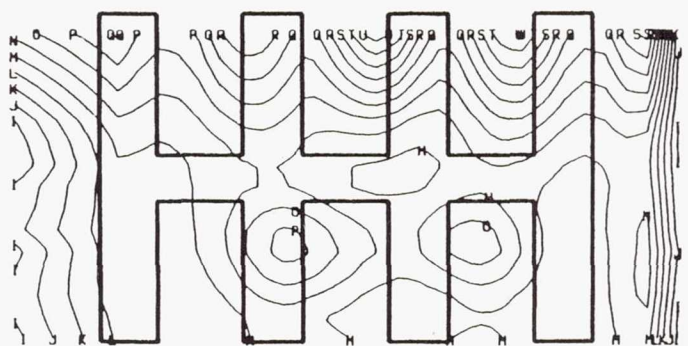
(a) Wing position 1.

(b) Wing position 5.

Figure 15.—Nondimensional total temperature nozzle exit contours for top long shroud at NPR=2.5.



(a)

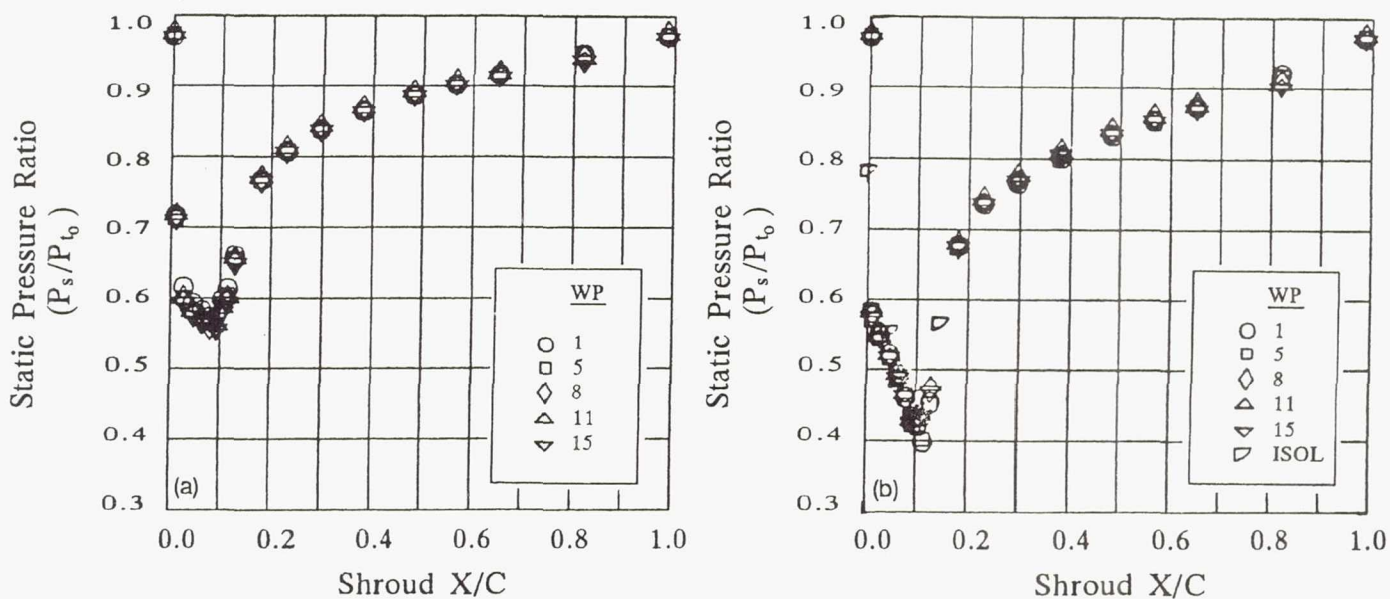


(b)

(a) Wing position 1.

(b) Wing position 5.

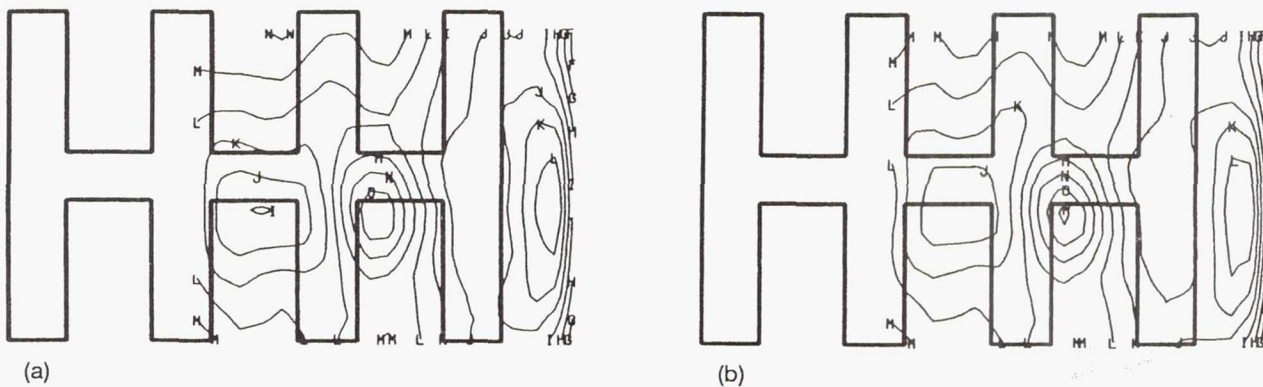
Figure 16.—Nondimensional total temperature nozzle exit contours for top long shroud at NPR=3.5.



(a) NPR=2.5.
(b) NPR=3.5.

Figure 17.—Short-top-shroud static pressure for five wing positions.

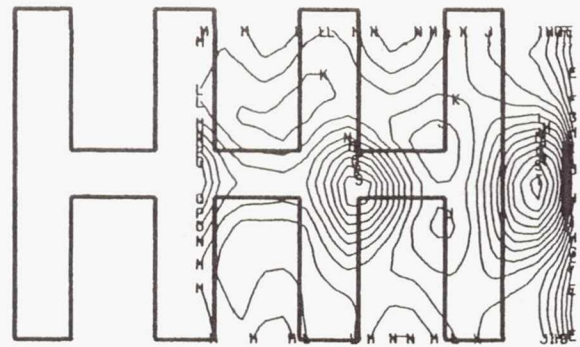
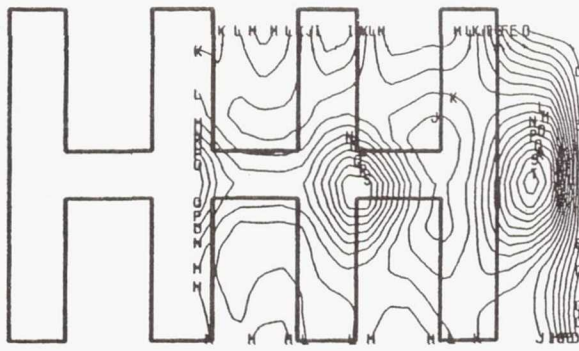
CONTOUR LABEL	CONTOUR VALUE				
A	0.00	G	0.24	M	0.48
B	0.04	H	0.28	N	0.52
C	0.08	I	0.32	O	0.56
D	0.12	J	0.36	P	0.60
E	0.16	K	0.40	Q	0.64
F	0.20	L	0.44	R	0.68
				S	0.72
				T	0.76
				U	0.80
				V	0.84
				W	0.88
				X	0.92
				Y	0.96
				Z	1.00



(a) Wing position 1.
(b) Wing position 5.

Figure 18.—Nondimensional total temperature nozzle exit contours for short top shroud at NPR=2.5.

CONTOUR LABEL		CONTOUR VALUE		M	0.48	T	0.76
A	0.00	G	0.24	N	0.52	U	0.80
B	0.04	H	0.28	O	0.56	V	0.84
C	0.08	I	0.32	P	0.60	W	0.88
D	0.12	J	0.36	Q	0.64	X	0.92
E	0.16	K	0.40	R	0.68	Y	0.96
F	0.20	L	0.44	S	0.72	Z	1.00



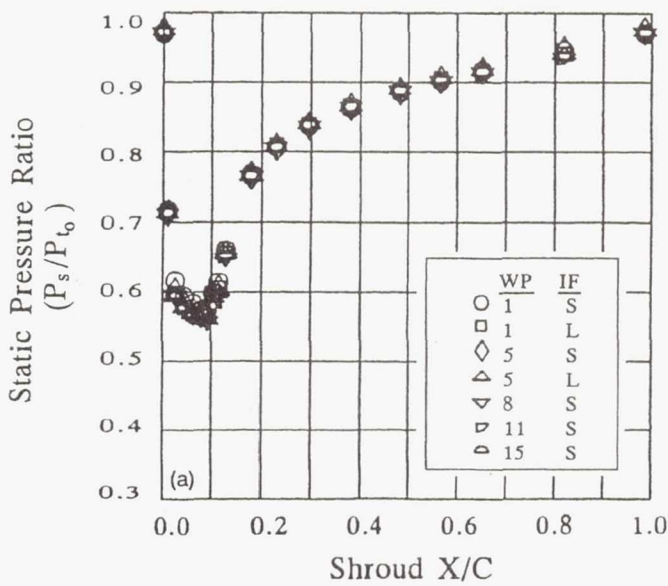
(a)

(b)

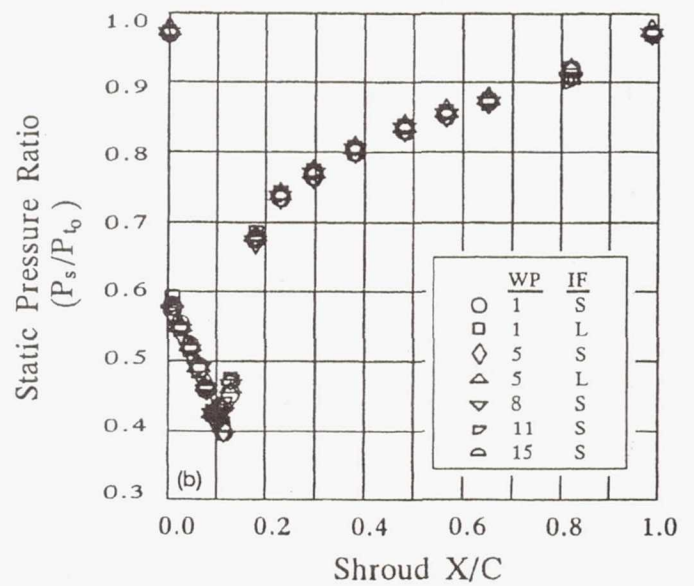
(a) Wing position 1.

(b) Wing position 5.

Figure 19.—Nondimensional total temperature nozzle exit contours for short top shroud at NPR=3.5



(a)

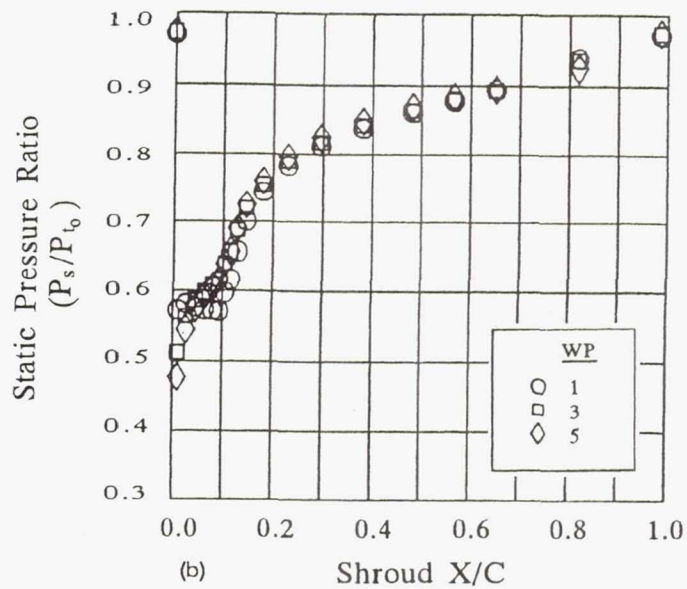
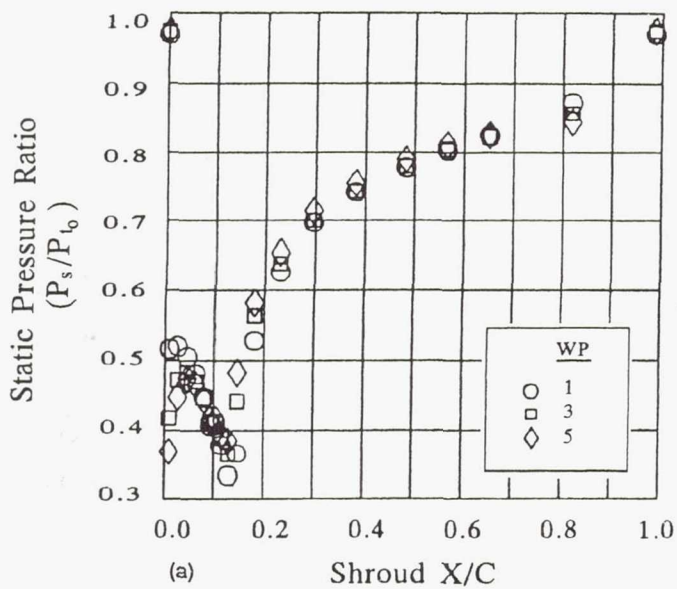


(b)

(a) NPR=2.5.

(b) NPR=3.5.

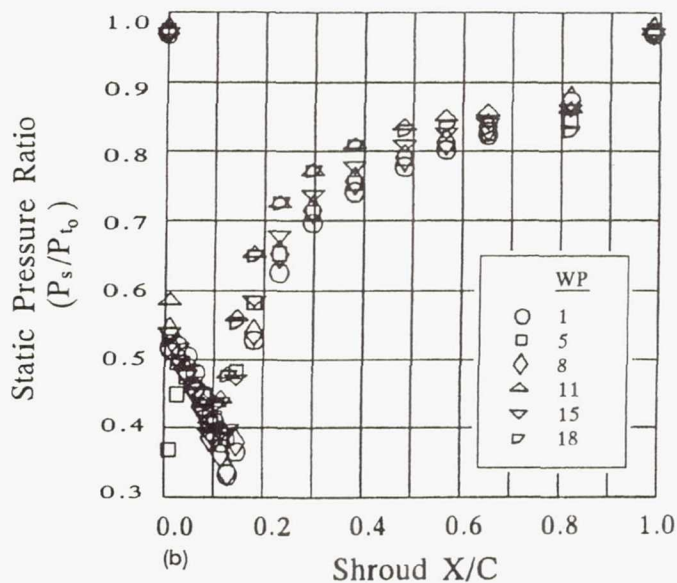
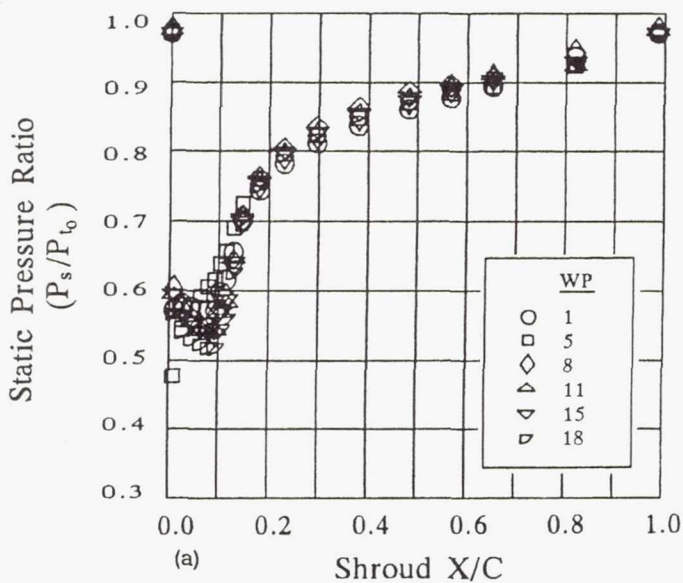
Figure 20.—Evaluation of interfering length on short-top-shroud static pressures.



(a) NPR=2.5.

(b) NPR=3.5.

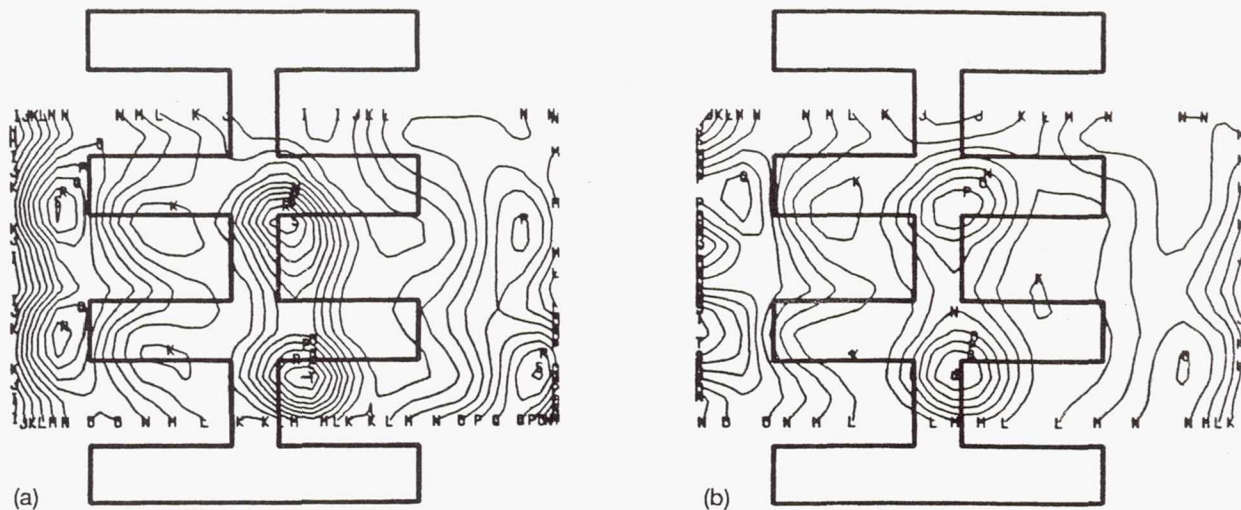
Figure 21.—Effect of 20/40 flaps on short-inboard-shroud static pressures.



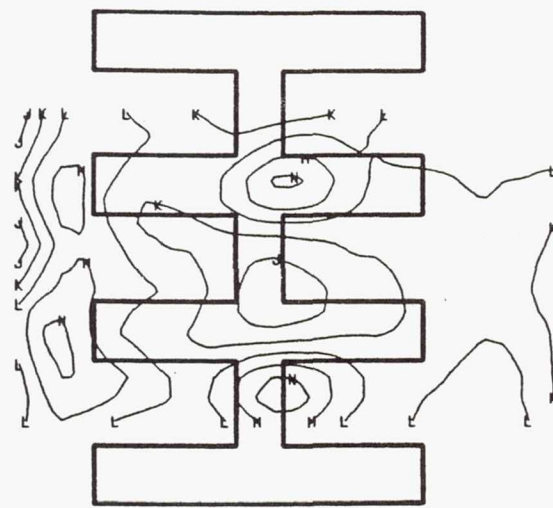
(a) NPR=2.5.

(b) NPR=3.5.

Figure 22.—Effect of wing position with 20/40 flaps on short-inboard-shroud static pressures.

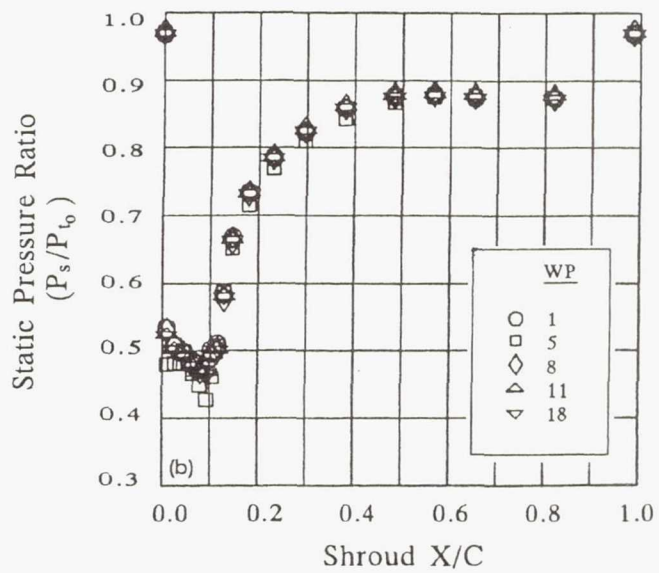
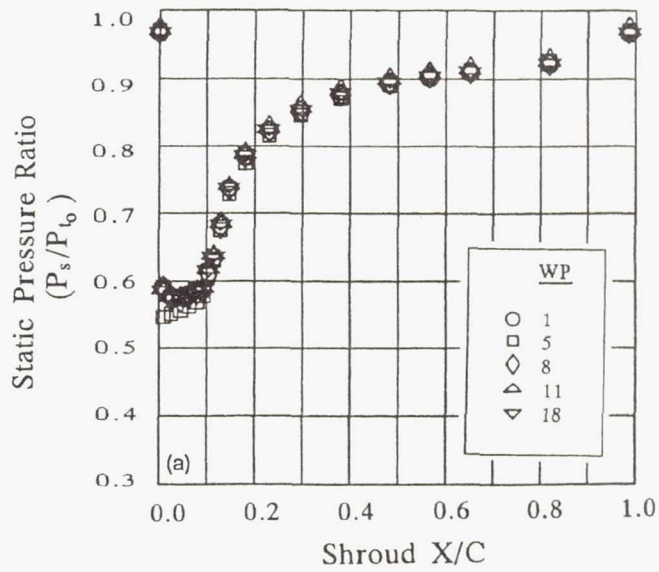


CONTOUR LABEL	CONTOUR VALUE
A	0.00
B	0.04
C	0.08
D	0.12
E	0.16
F	0.20
G	0.24
H	0.28
I	0.32
J	0.36
K	0.40
L	0.44
M	0.48
N	0.52
O	0.56
P	0.60
Q	0.64
R	0.68
S	0.72
T	0.76
U	0.80
V	0.84
W	0.88
X	0.92
Y	0.96
Z	1.00



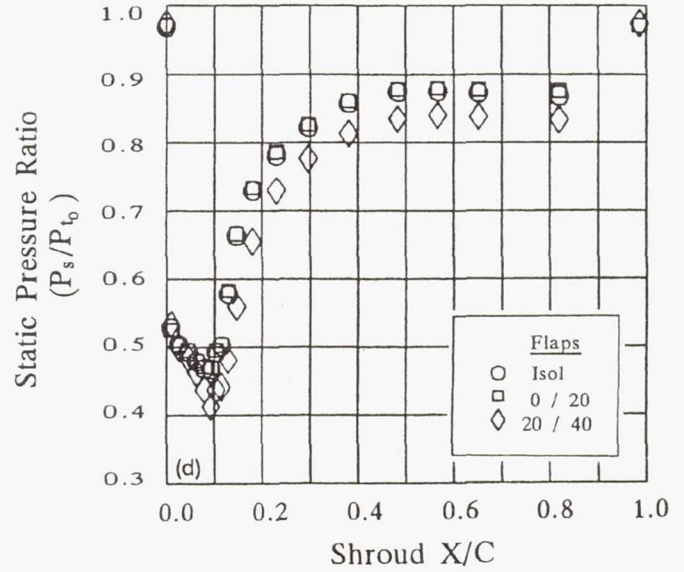
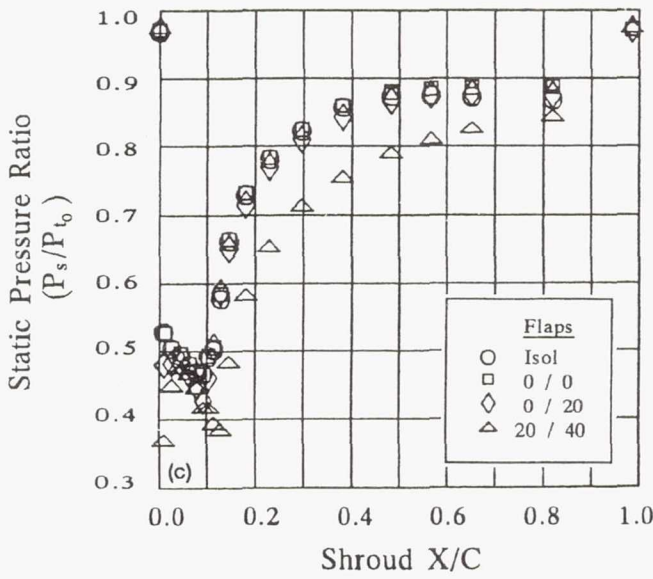
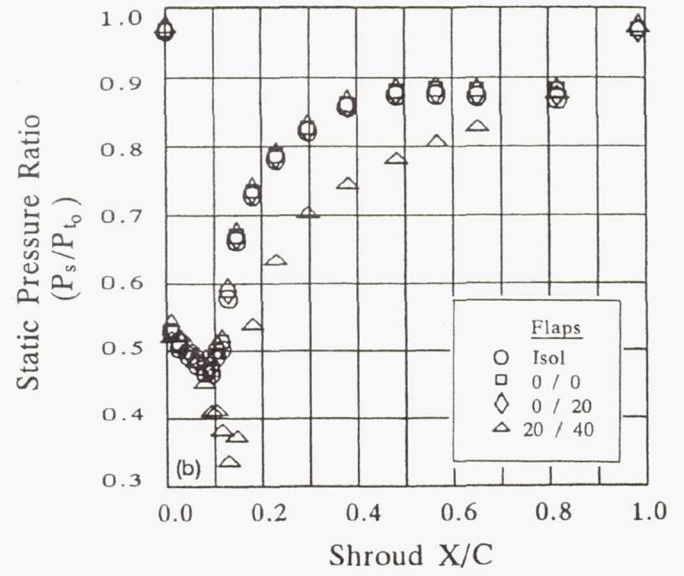
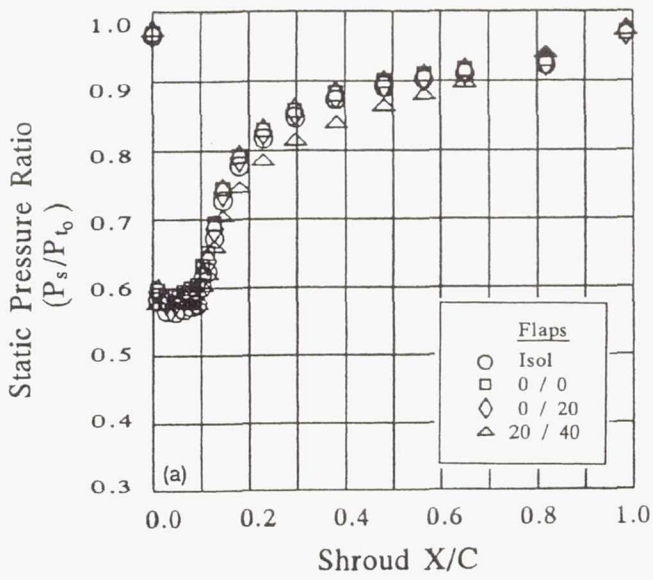
- (a) Wing position 1; NPR=3.5.
- (b) Wing position 5; NPR=3.5.
- (c) Wing position 5; NPR=2.5.

Figure 23.—Nondimensional total temperature nozzle exit contours with 20/40 flaps.



(a) NPR=2.5.
 (b) NPR=3.5.

Figure 24.—Effect of 0/20 flaps on short-inboard-shroud static pressures.



(a) Wing position 1; NPR=2.5.

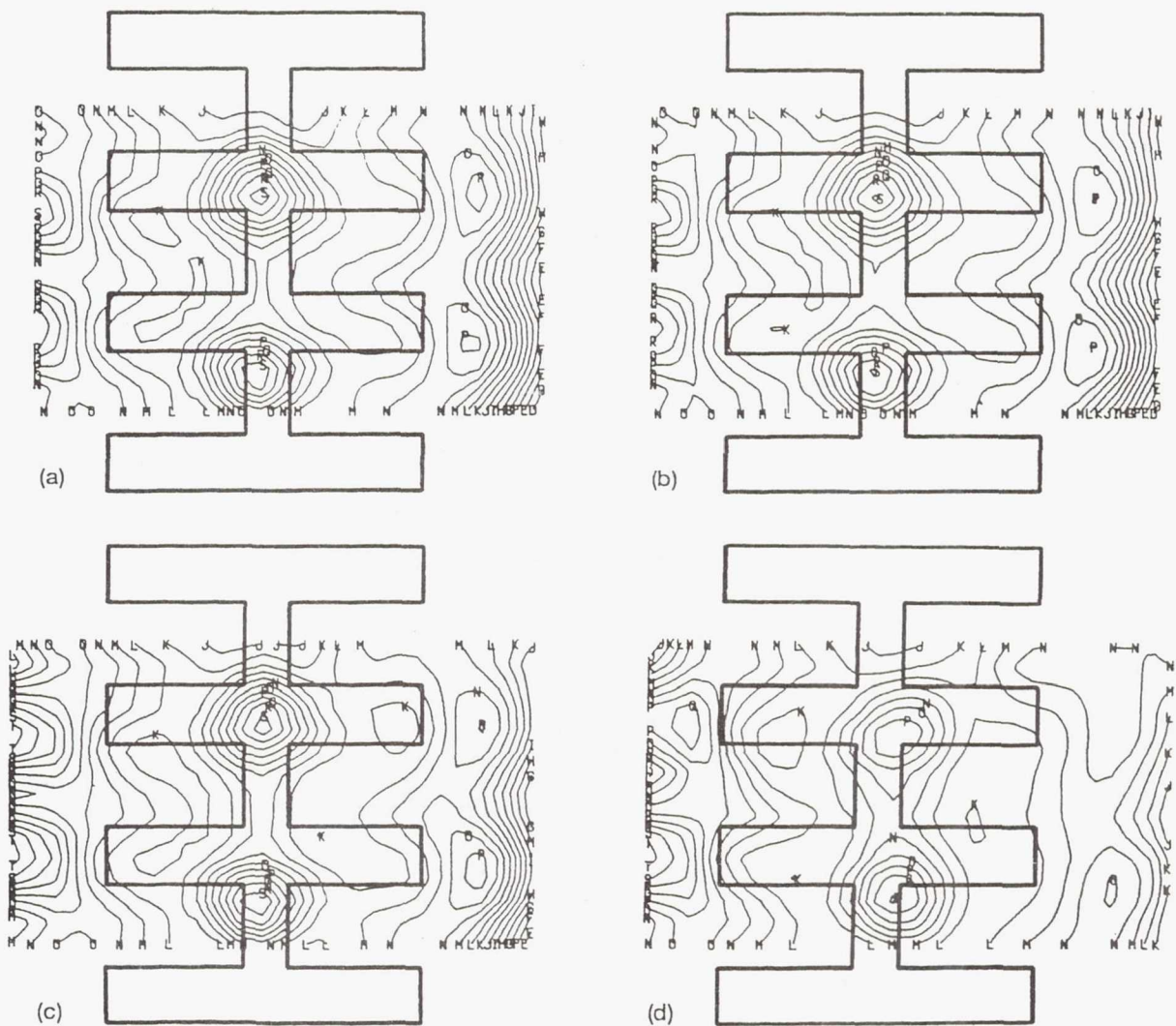
(b) Wing position 1; NPR=3.5.

(c) Wing position 5; NPR=3.5.

(d) Wing position 18; NPR=3.5.

Figure 25.—Effect of flap setting on short-inboard-shroud pressures.

CONTOUR LABEL		CONTOUR VALUE			
A	0.00	G	0.24	M	0.48
B	0.04	H	0.28	N	0.52
C	0.08	I	0.32	O	0.56
D	0.12	J	0.36	P	0.60
E	0.16	K	0.40	Q	0.64
F	0.20	L	0.44	R	0.68
				S	0.72
				T	0.76
				U	0.80
				V	0.84
				W	0.88
				X	0.92
				Y	0.96
				Z	1.00



- (a) Isolated nozzle.
- (b) Wing position 5 with 0/0 flaps.
- (c) Wing position 5 with 0/20 flaps.
- (d) Wing position 5 with 20/40 flaps.

Figure 26.—Nondimensional total temperature nozzle exit contours at NPR=3.5.

REPORT DOCUMENTATION PAGE

Form Approved
OMB No. 0704-0188

Public reporting burden for this collection of information is estimated to average 1 hour per response, including the time for reviewing instructions, searching existing data sources, gathering and maintaining the data needed, and completing and reviewing the collection of information. Send comments regarding this burden estimate or any other aspect of this collection of information, including suggestions for reducing this burden, to Washington Headquarters Services, Directorate for Information Operations and Reports, 1215 Jefferson Davis Highway, Suite 1204, Arlington, VA 22202-4302, and to the Office of Management and Budget, Paperwork Reduction Project (0704-0188), Washington, DC 20503.

1. AGENCY USE ONLY (Leave blank)	2. REPORT DATE 1992	3. REPORT TYPE AND DATES COVERED Technical Memorandum	
4. TITLE AND SUBTITLE Experimental Investigation of Wing Installation Effects on a Two-Dimensional Mixer/Ejector Nozzle for Supersonic Transport Aircraft		5. FUNDING NUMBERS WU-537-02-23	
6. AUTHOR(S) David J. Anderson, Heather H. Lambert, and Masashi Mizukami		7. PERFORMING ORGANIZATION NAME(S) AND ADDRESS(ES) National Aeronautics and Space Administration Lewis Research Center Cleveland, Ohio 44135-3191	
8. PERFORMING ORGANIZATION REPORT NUMBER E-7107		9. SPONSORING/MONITORING AGENCY NAMES(S) AND ADDRESS(ES) National Aeronautics and Space Administration Washington, D.C. 20546-0001	
10. SPONSORING/MONITORING AGENCY REPORT NUMBER NASA TM-105713		11. SUPPLEMENTARY NOTES	
12a. DISTRIBUTION/AVAILABILITY STATEMENT LIMITED DISTRIBUTION DOCUMENT Because of its significant technological potential, this information which has been developed under a U.S. Government program is being given a limited distribution whereby advanced access is provided for use by domestic interests. This legend shall be marked on any reproduction of this information in whole or in part. Date for general release <u>July 30, 1995</u> Subject Category 02		12b. DISTRIBUTION CODE	
13. ABSTRACT (Maximum 200 words) This report presents experimental results from a wind tunnel test conducted to investigate propulsion/air frame integration (PAI) effects. The objectives of the test were to examine rough order-of-magnitude changes to the acoustic characteristics of a mixer/ejector nozzle due to the presence of a wing and to obtain limited wing and nozzle flow-field measurements. A simple representative supersonic transport wing plan form, with deflecting flaps, was installed above a two-dimensional mixer/ejector nozzle that was supplied with high-pressure heated air. Various configurations and wing positions with respect to the nozzle were studied. Because of hardware problems, no acoustics and only a limited set of flow-field data were obtained. For most hardware configurations tested, no significant propulsion/air frame integration effects were identified. Significant effects were seen for extreme flap deflections. The combination of the exploratory nature of the test and the limited flow-field instrumentation made it impossible to identify definitive propulsion/air frame integration effects.			
14. SUBJECT TERMS Engine airframe integration; Propulsion airframe integration; Mixer nozzle; Ejector nozzle supersonic transport		15. NUMBER OF PAGES 30	
16. PRICE CODE A03		17. SECURITY CLASSIFICATION OF REPORT Unclassified	
18. SECURITY CLASSIFICATION OF THIS PAGE Unclassified		19. SECURITY CLASSIFICATION OF ABSTRACT Unclassified	
20. LIMITATION OF ABSTRACT			